

# Enhanced Crystallization Behaviour and Microwave Dielectric Properties of $0.9\text{CaMgSi}_2\text{O}_6\text{-}0.1\text{MgSiO}_3$ Glass-Ceramics Doped with $\text{TiO}_2$

Hyun Jin Jo, Gui Nam Sun, and Eung Soo Kim<sup>†</sup>

Department of Materials Engineering, Kyonggi University, Suwon 16227, Korea

(Received February 1, 2016; Revised February 18, 2016; Accepted February 19, 2016)

## ABSTRACT

The dependence of the microwave dielectric properties of the glass-ceramic composite  $0.9\text{CaMgSi}_2\text{O}_6\text{-}0.1\text{MgSiO}_3$  on the crystallization behaviour was investigated as functions of the  $\text{TiO}_2$  content and heat-treatment temperature. The crystallization behaviour of the specimens was evaluated via a combination of the Rietveld and reference-intensity ratio methods. For specimens with a  $\text{TiO}_2$  content of up to 1 wt.%, a monoclinic diopside phase was formed, whereas a secondary  $\text{TiO}_2$  phase was formed with further increases in the  $\text{TiO}_2$  content. The quality factor ( $Qf$ ) of the specimens was strongly dependent on the degree of crystallization. The highest  $Qf$  value was obtained with a  $\text{TiO}_2$  content of 0.5 wt.%, which was improved by increasing the heat-treatment temperature. The dielectric constant ( $K$ ) was affected by the size of the crystallites and the  $\text{TiO}_2$  content. The temperature coefficient of the resonant frequency ( $TCF$ ) was nearly constant for all of the specimens, regardless of the  $\text{TiO}_2$  content or heat-treatment temperature.

**Key words :** Glass-ceramics, Diopside, Enstatite, Microwave dielectric properties, Degree of crystallization

## 1. Introduction

In recent years, the applicability of low-temperature co-fired ceramics (LTCCs) to technology has been widely investigated to meet the demand for miniaturized and multifunctional electronic devices. The key properties required for LTCC-based substrate materials include a low dielectric constant ( $K$ ), high quality factor ( $Qf$ ), near-zero temperature coefficient of the resonant frequency ( $TCF$ ), and heat-treatment temperature that is much lower than the melting points of commonly used metallic electrodes (Ag, Au, or Cu).<sup>1)</sup>

$\text{CaMgSi}_2\text{O}_6$  and  $\text{MgSiO}_3$  (diopside and enstatite, respectively) glass-ceramic composites are good candidates for LTCC-based substrate materials because of the low heat-treatment temperature, low  $K$ , high  $Qf$ , and high mechanical strength of such systems.<sup>2)</sup> It has been reported that the dielectric properties of glass-ceramic composites can be affected by the density, porosity, crystalline phases formed, and degree of crystallization.<sup>3)</sup> According to our preliminary experiments, the glass-ceramic composite  $0.9\text{CaMgSi}_2\text{O}_6\text{-}0.1\text{MgSiO}_3$  exhibits a high  $Qf$  value (36,000 GHz) when a high degree of crystallization is achieved.<sup>2)</sup> Therefore, improving the degree of crystallization of  $0.9\text{CaMgSi}_2\text{O}_6\text{-}0.1\text{MgSiO}_3$  is the most important factor for enhancing the  $Qf$  value.

Various methods have been developed to improve the

crystallization behaviour of glass-ceramic composites. One such method is controlling the heat-treatment temperature.<sup>2,4,5)</sup> Generally, glass-ceramic composites that are heat-treated at the optimum temperature exhibit enhanced crystallinity.<sup>5)</sup>

Another method for improving the crystallization of glass-ceramic composites is the addition of nucleation agents. With the addition of a nucleation agent, the crystallization of the glass can occur at both the surface and bulk, which can lead to an increase in the degree of crystallization;  $\text{Cr}_2\text{O}_3$  and  $\text{TiO}_2$  have been widely investigated as nucleation agents for the  $\text{CaMgSi}_2\text{O}_6$  system.<sup>4,6-11)</sup>

$\text{Cr}_2\text{O}_3$  is commonly used as a nucleation agent for diopside glass. It has been reported that the addition of  $\text{Cr}_2\text{O}_3$  leads to the formation of heterogeneous nucleation sites in diopside glass; this process causes crystallization via the formation of  $\text{MgCr}_2\text{O}_4$  spinel domains.<sup>7)</sup> However, Cr ions can exist in two valence states:  $\text{Cr}^{3+}$  and  $\text{Cr}^{6+}$ .<sup>8)</sup> It has been reported that  $\text{Cr}^{3+}$  is miscible with diopside glass at high temperatures, while  $\text{Cr}^{6+}$  separates from the diopside glass at low temperatures because of the high field strength of the hexavalent state. These phenomena can degrade the degree of crystallization of a diopside glass.<sup>9)</sup> Therefore,  $\text{Cr}_2\text{O}_3$  should be used alongside other nucleation agents for diopside glass, such as  $\text{Fe}_2\text{O}_3$  or  $\text{TiO}_2$ .<sup>4)</sup> On the other hand,  $\text{TiO}_2$  is a well-known nucleation agent for diopside glass. It can enter the glass as either a network modifier in the form of  $\text{TiO}_6$  at high temperatures, or as a network former in the form of  $\text{TiO}_4$  at low temperatures. Once  $\text{TiO}_2$  has been transformed into  $\text{TiO}_6$ , it can decrease the viscosity of the glass, thereby increasing the mobility during crystalliza-

<sup>†</sup>Corresponding author : Eung Soo Kim

E-mail : eskim@kyonggi.ac.kr

Tel : +82-31-249-9764 Fax : +82-31-244-6300

tion. Therefore, the addition of  $\text{TiO}_2$  can enhance the crystallization behaviour of diopside glass.<sup>10,11</sup> Thus, it is expected that the crystallinity of diopside glass can be improved by adding an optimum concentration of  $\text{TiO}_2$ .

Even though many studies have investigated the effects of  $\text{TiO}_2$  on glass-ceramic composites, the two factors controlling the degree of crystallization have not been sufficiently clarified, i.e., the optimum concentration of  $\text{TiO}_2$  for glass-ceramic composites and the relationship between the dielectric properties and the degree of crystallization have not been reported. Moreover, the effects of the  $\text{TiO}_2$  content and the heat-treatment temperature on the crystallization behaviour of  $0.9\text{CaMgSi}_2\text{O}_6\text{-}0.1\text{MgSiO}_3$  have not yet been investigated. Therefore, in this study, the microwave dielectric properties of  $0.9\text{CaMgSi}_2\text{O}_6\text{-}0.1\text{MgSiO}_3$  were investigated as functions of the  $\text{TiO}_2$  content (0-6 wt.%) and the heat-treatment temperature. The crystallization behaviour of the specimens will be discussed based on how the degree of crystallization varies with the  $\text{TiO}_2$  content and the heat-treatment temperature.

## 2. Experimental Procedures

$\text{CaCO}_3$  (99.9%),  $\text{MgCO}_3$  (99.9%),  $\text{SiO}_2$  (99.9%), and  $\text{TiO}_2$  (99.9%) powders were used as the precursor materials. The powders were mixed to achieve the desired composition of  $0.9\text{CaMgSi}_2\text{O}_6\text{-}0.1\text{MgSiO}_3$ , with the  $\text{TiO}_2$  content ranging from 0 to 6 wt.%; samples were ball-milled with  $\text{ZrO}_2$  balls for 24 h in ethanol. The mixed powders were then melted in Pt crucibles at  $1500^\circ\text{C}$  for 3 h and quenched in distilled water. Cullet of the samples was obtained by pulverizing the quenched products, which were then sieved through size-50 meshes. The glass frits were re-milled for 24 h and isostatically pressed into pellets at a pressure of 147 MPa. The pellets were then heat-treated at  $850\text{-}950^\circ\text{C}$  for 3 h in air.

The densities of the heat-treated specimens were measured via the Archimedes' method. The crystalline phases and crystallization behaviours of the specimens were analysed with X-ray diffraction (XRD, D/Max-2500V/PC, RIGAKU, Japan). Scanning electron microscopy (SEM, JSM-6700F, JEOL, Japan) was used to evaluate the phase and crystallite size of the glass-ceramic specimens.

To evaluate the degree of crystallization of the specimens via a combination of Rietveld and reference-intensity ratio (RIR) methods, a sample of 10 wt.%  $\alpha\text{-Al}_2\text{O}_3$ , which was annealed at  $1500^\circ\text{C}$  for 24 h to increase the crystallinity to 100%, was added to all of the samples to act as an internal standard.<sup>12,13</sup> Rietveld refinements of the XRD patterns were performed with the Full-Prof program.<sup>14</sup> The degree of crystallization of the samples was evaluated against the internal standard with Eq. (1):

$$\alpha = \left( \frac{W_c}{W_{std}} \right) \left( \frac{W_{std}}{W} \right) \quad (1)$$

where  $W$ ,  $W_c$ , and  $W_{std}$  are the weights of the specimen, crys-

talline component, and internal standard, respectively.<sup>12</sup> The value of  $W_c/W_{std}$  was calculated from the Rietveld quantitative analysis under the condition of  $W_c + W_{std} = 1$ . The value of  $W_{std}/W$  was determined by measuring the weights of the specimen and of the internal standard.<sup>13</sup> The microwave dielectric properties were measured according to the method reported by Hakki and Coleman with the  $\text{TE}_{011}$  mode in the range of 11-13 GHz.<sup>15</sup> The  $TCF$  values of the specimens were measured according to the cavity method over a temperature range of  $25\text{-}80^\circ\text{C}$ .<sup>16</sup>

## 3. Results and Discussion

### 3.1. Physical Properties

The relative densities of the  $0.9\text{CaMgSi}_2\text{O}_6\text{-}0.1\text{MgSiO}_3$  specimens with various  $\text{TiO}_2$  contents (0-6 wt.%) that were heat-treated at  $850\text{-}950^\circ\text{C}$  for 3 h are shown in Fig. 1. As the  $\text{TiO}_2$  content increases, the relative densities of all of the specimens decrease, but remain above 90% regardless of the  $\text{TiO}_2$  content.

Figure 2 provides SEM micrographs of the  $0.9\text{CaMgSi}_2\text{O}_6\text{-}0.1\text{MgSiO}_3$  specimens with  $\text{TiO}_2$  contents of 0.5, 2, and 6 wt.% that were heat-treated at  $850^\circ\text{C}$  for 3 h. As the  $\text{TiO}_2$  content increases, the porosity increases because of the decreasing relative density, as shown in Fig. 1. These results can be attributed to the weak adhesion at the interfaces between the diopside (glass) and  $\text{TiO}_2$  (ceramic) phases, which arises from the degradation of pore elimination during the densification process and/or the difference between the thermal expansion coefficients of the diopside ( $8.40 \times 10^6 \text{ }^\circ\text{C}^{-1}$  (crystal),  $6.65 \times 10^6 \text{ }^\circ\text{C}^{-1}$  (glass)<sup>17</sup>) and  $\text{TiO}_2$  phases ( $8.9210\text{-}60^\circ\text{C}^{-1}$ <sup>18</sup>). Considering the globular shape of the pores shown in Fig. 2, the degradation of pore elimination during the densification process is a major factor in the weak adhesion.

Figure 3 provides XRD patterns of the  $0.9\text{CaMgSi}_2\text{O}_6\text{-}0.1\text{MgSiO}_3$  specimens with various  $\text{TiO}_2$  contents (0-6 wt.%)

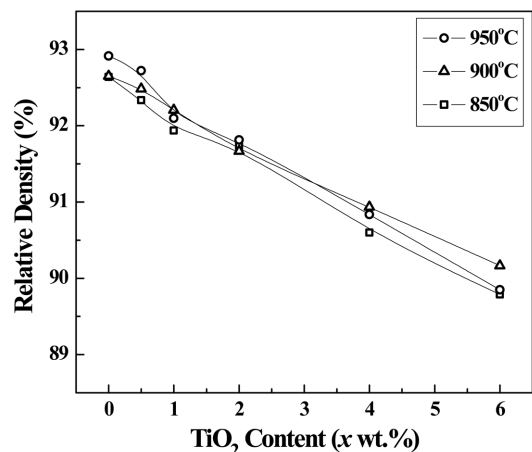
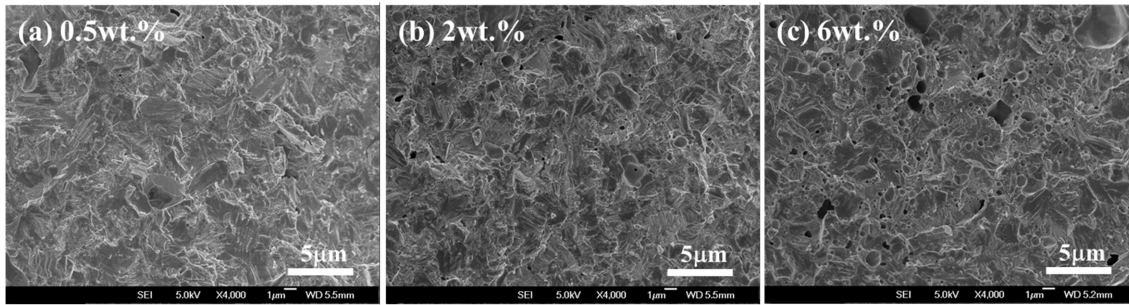
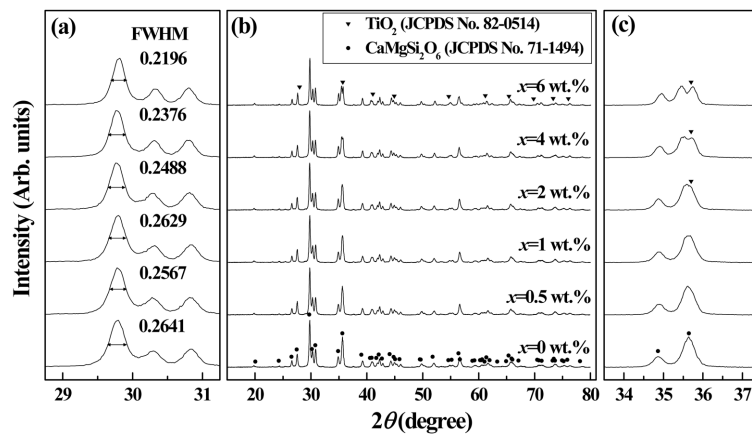


Fig. 1. Relative densities of the  $0.9\text{CaMgSi}_2\text{O}_6\text{-}0.1\text{MgSiO}_3$  specimens with various  $\text{TiO}_2$  contents (0-6 wt.%) that were heat-treated at  $850\text{-}950^\circ\text{C}$  for 3 h.



**Fig. 2.** SEM micrographs of the  $0.9\text{CaMgSi}_2\text{O}_6\text{-}0.1\text{MgSiO}_3$  specimens with various  $\text{TiO}_2$  contents (0.5-6 wt.%) that were heat-treated at  $850\text{-}950\text{ }^\circ\text{C}$  for 3 h: (a) 0.5, (b) 2, and (c) 6 wt.%.



**Fig. 3.** XRD patterns of the  $0.9\text{CaMgSi}_2\text{O}_6\text{-}0.1\text{MgSiO}_3$  specimens with various  $\text{TiO}_2$  contents (0-6 wt.%) that were heat-treated at  $850\text{ }^\circ\text{C}$  for 3 h: (a)  $2\theta = 29\text{-}31^\circ$ , (b)  $2\theta = 15\text{-}80^\circ$ , and (c)  $2\theta = 34\text{-}37^\circ$ .

that were heat-treated at  $850\text{ }^\circ\text{C}$  for 3 h. The XRD patterns show that a single monoclinic diopside phase ( $\text{CaMgSi}_2\text{O}_6$ , JCPDS No. 71-1494) is detected for  $\text{TiO}_2$  contents of up to 1 wt.% (Fig. 3(b)). However, a secondary  $\text{TiO}_2$  phase (JCPDS No. 82-0514) becomes evident with further increases in the  $\text{TiO}_2$  content; this is confirmed by the XRD peak at  $2\theta = 35.5^\circ$  splitting into the diopside and  $\text{TiO}_2$  phases (Fig. 3(c)).

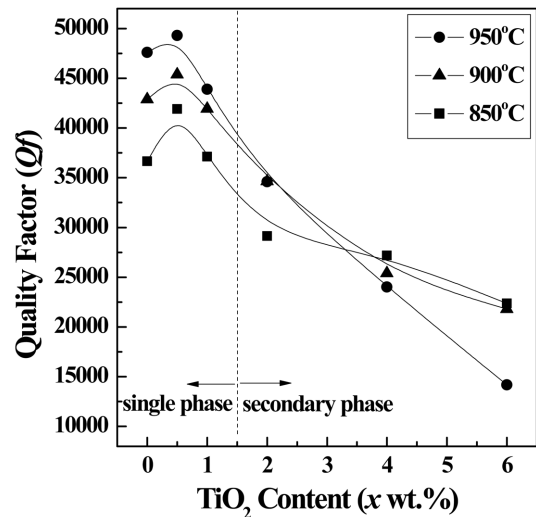
To determine the crystallite size ( $L$ ) of the specimens, the full width at half-maximum (FWHM) values of the XRD peaks were calculated with the Scherrer Equation (Eq. (2))<sup>19</sup>:

$$L = \frac{0.89\lambda}{B \cos \theta} \quad (2)$$

where  $L$  is the crystallite size,  $\lambda$  is the wavelength of the X-ray radiation ( $\lambda = 0.154\text{ nm}$ ),  $B$  is the FWHM of the peak (in radians) after being corrected for instrumental broadening, and  $\theta$  is the Bragg angle. As the FWHM of an XRD peak decreases, the crystallite size increases. Fig. 3(a) shows that the specimens containing less than 1 wt.% of  $\text{TiO}_2$  have similar FWHM values, while those with  $\text{TiO}_2$  contents greater than 1 wt.% exhibit reduced FWHM values, which indicates that the crystallite size has increased.

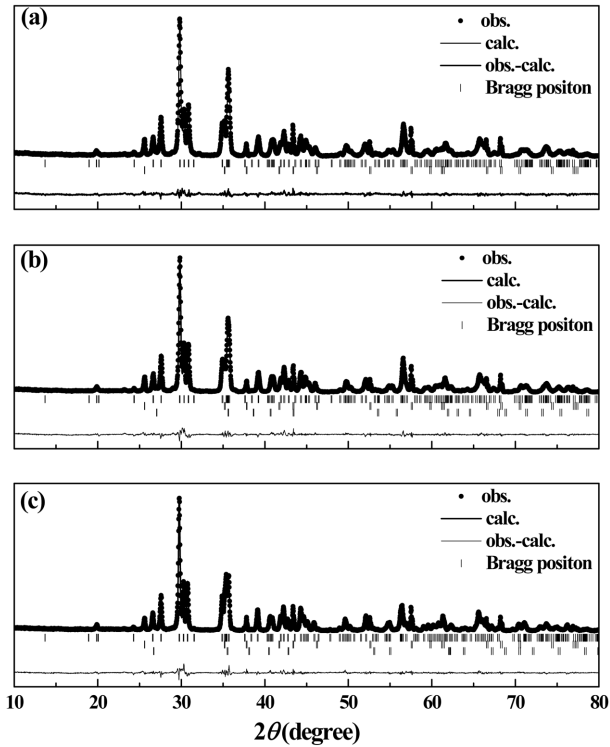
### 3.2. Microwave Dielectric Properties

Figure 4 shows the relationship between the  $Qf$  values of



**Fig. 4.** Quality factor ( $Qf$ ) values for the  $0.9\text{CaMgSi}_2\text{O}_6\text{-}0.1\text{MgSiO}_3$  specimens with various  $\text{TiO}_2$  contents (0-6 wt.%) that were heat-treated at  $850\text{-}950\text{ }^\circ\text{C}$  for 3 h.

the  $0.9\text{CaMgSi}_2\text{O}_6\text{-}0.1\text{MgSiO}_3$  specimens and the  $\text{TiO}_2$  content (0 - 6 wt.%), as well as the effects of the heat-treatment temperature on the  $Qf$  values. The maximum  $Qf$  value for each temperature is achieved when the  $\text{TiO}_2$  content is 0.5 wt.%, and then the  $Qf$  values gradually decrease with fur-



**Fig. 5.** Rietveld-refined patterns of the  $0.9\text{CaMgSi}_2\text{O}_6\text{-}0.1\text{MgSiO}_3$  specimens with various  $\text{TiO}_2$  contents (0.5-6 wt.%) that were heat-treated at 850-950°C for 3 h: (a) 0.5, (b) 2, and (c) 6 wt.%.

ther increases in the  $\text{TiO}_2$  content. In addition, the  $Qf$  values increase as the heat-treatment temperature increases from 850 to 950°C. Generally, the  $Qf$  value of a glass-ceramic composite is strongly dependent on the degree of crystallization, which can be improved by either adding a nucleation agent, such as  $\text{TiO}_2$ , or increasing the heat-treatment temperature.

To evaluate the crystallinity of the  $0.9\text{CaMgSi}_2\text{O}_6\text{-}0.1\text{MgSiO}_3$  specimens with various  $\text{TiO}_2$  contents (0-6 wt.%) that were subjected to heat treatments at different temperatures, the Rietveld-RIR method described in section 2 was used. The resulting Rietveld-refined patterns are shown in

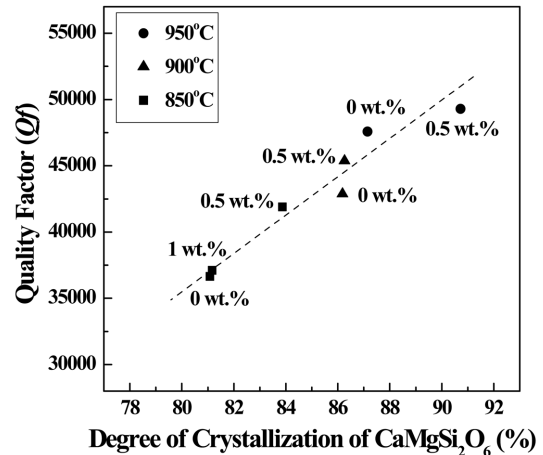


**Fig. 6.** Dependence of the quality factor ( $Qf$ ) on the degree of crystallization of the  $0.9\text{CaMgSi}_2\text{O}_6\text{-}0.1\text{MgSiO}_3$  specimens with various  $\text{TiO}_2$  contents (0-1 wt.%) that were heat-treated at 850-950°C for 3 h.

Fig. 5. The data points represent the measured intensities, the overlying solid lines are the calculated intensities, and the lower lines show the differences between the observed and calculated intensities. In addition, the short vertical bars indicate the Bragg reflections that correspond to the monoclinic diopside (top row),  $\alpha\text{-Al}_2\text{O}_3$  (middle row), and  $\text{TiO}_2$  (bottom row) phases. Table 1 shows that the  $R$ -factors, i.e. the goodness of fit ( $GoF$ ), profile factor ( $R_p$ ), weighted profile factor ( $R_{wp}$ ), and expected weighted profile factor ( $R_{exp}$ ), have low values, indicating that the Rietveld-refined results are reliable.

Figure 6 shows the dependence of the  $Qf$  values on the degree of crystallization of the glass-ceramic composites. For the specimens composed of a single diopside phase ( $\text{TiO}_2$  content = 0-1 wt.%), the highest degree of crystallization is obtained with a  $\text{TiO}_2$  content of 0.5 wt.%; the crystallization then decreases and is nearly constant with further increases in the  $\text{TiO}_2$  content, as shown in Table 1. In addition, the degree of crystallization of the specimens with  $\text{TiO}_2$  contents of 0.5 wt.% is enhanced as the heat-treatment temperature increases from 850 to 950°C. These tendencies are reflected

**Table 1.** Results of the Rietveld-RIR Quantitative Analysis of the  $0.9\text{CaMgSi}_2\text{O}_6\text{-}0.1\text{MgSiO}_3$  Specimens with Various  $\text{TiO}_2$  Contents (0-6 wt.%) that were Heat-Treated at 850-950°C for 3 h

$\text{TiO}_2$ (wt.%)	0	0.5	1	2	4	6		
Heat-treatment temperature (°C)	850	850	900	950	850			
Degree of crystallization of $\text{CaMgSi}_2\text{O}_6$ (%)	81.79	83.87	86.25	87.15	81.17	79.36	81.64	80.20
$\text{TiO}_2$ (%)	0	0	0	0	0	0.35(4)	0.65(2)	0.77(7)
Glass (%)	18.21	16.13	13.75	12.85	18.83	20.29	17.71	19.03
Total (%)	100.00	100.00	100.00	100.00	100.00	99.9	99.9	99.9
$GoF$	1.6	1.5	1.5	1.5	1.5	1.6	1.5	1.5
$R_p$	8.71	8.26	8.35	8.54	8.6	9.02	9.09	9.52
$R_{wp}$	11.1	10.4	10.5	10.7	10.9	11.4	11.2	11.6
$R_{exp}$	7.1	7.01	6.99	7.12	7.12	7.09	7.23	7.26

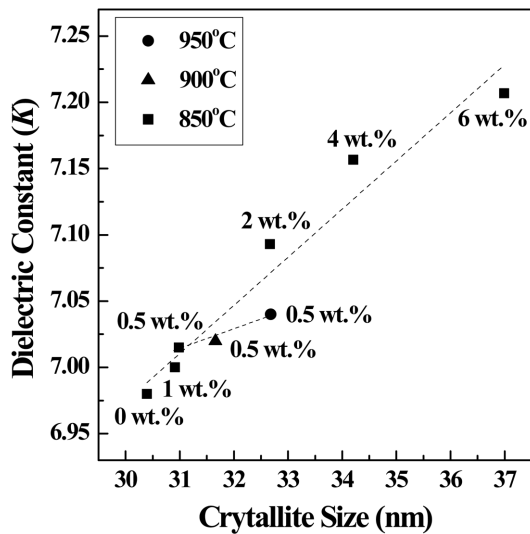


Fig. 7. Dependence of the dielectric constant ( $K$ ) on the crystallite size of the  $0.9\text{CaMgSi}_2\text{O}_6\text{-}0.1\text{MgSiO}_3$  specimens with various  $\text{TiO}_2$  contents (0-6 wt.%) that were heat-treated at 850-950°C for 3 h.

in the trends of the  $Qf$  values of the specimens, as shown in Fig. 4. This is because single crystals always have smaller dielectric losses than the corresponding glass and, thus, high  $Qf$  values of the specimens are obtained when there is a high degree of crystallization.<sup>20</sup> In addition, the  $Qf$  value of the specimen containing 0.5 wt.% of  $\text{TiO}_2$  and heat-treated at 950°C ( $Qf = 49,300$  GHz) is similar to that of the  $\text{CaMgSi}_2\text{O}_6$  ceramics sintered at 1290°C ( $Qf = 59,600$  GHz<sup>21</sup>), but the dielectric properties are not highly degraded because of the lower heat-treatment temperature.

Figure 7 shows the dependence of  $K$  on the crystallite size of the  $0.9\text{CaMgSi}_2\text{O}_6\text{-}0.1\text{MgSiO}_3$  specimens with various  $\text{TiO}_2$  contents (0-6 wt.%) that were heat-treated at 850-950°C for 3 h. The crystallite sizes of the specimens are similar for  $\text{TiO}_2$  contents of up to 1 wt.%; then, the crystallite sizes increase from 30.8 to 37.0 nm with further increases in the  $\text{TiO}_2$  content, as shown in Fig. 3(a). The crystallite size increases with increasing  $\text{TiO}_2$  content because of the accelerated grain growth that is caused by heterogeneous nucleation.<sup>22</sup> For the specimens with  $\text{TiO}_2$  contents of 0.5 wt.%, the crystallite size also increases as the heat-treatment temperature increases from 850 to 950°C. It has been reported that  $K$  is dependent on the crystallite size of the specimens because of the reduced porosity of the interfaces between the grains.<sup>3,23,24</sup> In addition, the increasing  $K$  values of the specimens could be caused by the higher intrinsic  $K$  of the secondary  $\text{TiO}_2$  phase ( $K_{\text{TiO}_2} = 100$ <sup>25</sup>), while  $K = 6.98$  for the  $0.9\text{CaMgSi}_2\text{O}_6\text{-}0.1\text{MgSiO}_3$  phase).

The  $TCF$  values of the  $0.9\text{CaMgSi}_2\text{O}_6\text{-}0.1\text{MgSiO}_3$  specimens with various  $\text{TiO}_2$  contents (0-6 wt.%) that were heat-treated at 850-950°C for 3 h did not change significantly with the  $\text{TiO}_2$  content and/or heat-treatment temperature; the  $TCF$  values were approximately -20 ppm/°C for all of the compositions tested.

## 4. Conclusions

In this study, the effects of the  $\text{TiO}_2$  content (0-6 wt.%) and heat-treatment temperature on the microwave dielectric properties of  $0.9\text{CaMgSi}_2\text{O}_6\text{-}0.1\text{MgSiO}_3$  glass-ceramic composites were investigated. The specimens with  $\text{TiO}_2$  contents of up to 1 wt.% and heat-treated at 850°C for 3 h exhibited a single phase of diopside ( $\text{CaMgSi}_2\text{O}_6$ ), and then a secondary  $\text{TiO}_2$  phase became evident with further increases in the  $\text{TiO}_2$  content. For the specimens composed of a single diopside phase, the  $Qf$  values of these specimens were dependent on the degree of crystallization, which was affected by both the  $\text{TiO}_2$  content and the heat-treatment temperature; the highest degree of crystallization was achieved when the  $\text{TiO}_2$  content was 0.5 wt.%. Moreover, the degree of crystallization of the specimens with  $\text{TiO}_2$  contents of 0.5 wt.% was improved by increasing the heat-treatment temperature. The  $K$  values of the specimens were mainly affected by the size of the crystallites, while the  $TCF$  values did not change significantly. By adding 0.5 wt.% of  $\text{TiO}_2$  to the  $0.9\text{CaMgSi}_2\text{O}_6\text{-}0.1\text{MgSiO}_3$  glass-ceramic composite ( $Qf = 49,300$  GHz), the heat-treatment temperature was effectively lowered to 950°C.

## REFERENCES

1. E. S. Kim, S. H. Kim, and B. I. Lee, "Low-Temperature Sintering and Microwave Dielectric Properties of  $\text{CaWO}_4$  Ceramics for LTCC Applications," *J. Eur. Ceram. Soc.*, **26** [10-11] 2101-4 (2006).
2. G. N. Sun and E. S. Kim, "Microwave Dielectric Properties of Diopside-Enstatite Glass-Ceramics," *Ferroelectrics*, **434** [1] 44-51 (2012).
3. J. H. Kim, S. J. Hwang, W. K. Sung, and H. S. Kim, "Thermal and Dielectric Properties of Glass-Ceramics Sintered Based on Diopside and Anorthite Composition," *J. Electroceram.*, **23** [2] 209-13 (2009).
4. Y. J. Eoh and E. S. Kim, "Effect of Heat-Treatment on the Dielectric Properties of  $\text{CaMgSi}_2\text{O}_6$  Glass-Ceramics with  $\text{Cr}_2\text{O}_3\text{-Fe}_2\text{O}_3\text{-TiO}_2$ ," *Jpn. J. Appl. Phys.*, **53** [8S3] 08NB01 (2014).
5. X. Zheng, G. Wen, L. Song, and X. X. Huang, "Effects of  $\text{P}_2\text{O}_5$  and Heat Treatment on Crystallization and Microstructure in Lithium Disilicate Glass Ceramics," *Acta Mater.*, **56** [17] 549-58 (2008).
6. L. Barbieri, C. Leonelli, T. Manfredini, G. C. Pellacani, C. Siligardi, E. Tondello, and R. Bertinello, "Solubility, Reactivity and Nucleation Effect of  $\text{Cr}_2\text{O}_3$  in the  $\text{CaO-MgO-Al}_2\text{O}_3\text{-SiO}_2$  Glassy System," *J. Mater. Sci.*, **29** [23] 6273-80 (1994).
7. J. Williamson, "The Kinetics of Crystal Growth in an Aluminosilicate Glass Containing Small Amounts of Transition-Metal Ions," *Mineral. Mag.*, **37** [291] 759-70 (1970).
8. T. Murata, M. Torisaka, H. Takebe, and K. Morinaga, "Compositional Dependence of the Valency State of Cr Ions in Oxide Glasses," *J. Non-Cryst. Solids*, **220** [2-3] 139-46 (1997).
9. A. A. Omar, S. M. Salman, and M. Y. Mahmoud, "Cata-

- lyzed Crystallization of Various Glasses Based on Sedimentary Rock Mixtures," *Ceramurgia*, **15** [2] 57 (1985).
10. R. G. Duan, K. M. Liang, and S. R. Gu, "Effect of Changing TiO<sub>2</sub> Content on Structure and Crystallization of CaO-Al<sub>2</sub>O<sub>3</sub>-SiO<sub>2</sub> System Glasses," *J. Eur. Ceram. Soc.*, **18** [12] 1729-35 (1998).
  11. V. M. F. Marques, D. U. Tulyaganov, G. P. Kothiyal, J. M. F. Ferreira, "The Effect of TiO<sub>2</sub> and P<sub>2</sub>O<sub>5</sub> on Densification Behavior and Properties of Anortite-Diopside Glass-Ceramic Substrates," *J. Electroceram.*, **25** [1] 38-44 (2010).
  12. K. Yasukawa, Y. Terashi, and A. Nakayama, "Crystallinity Analysis of Glass-Ceramics by the Rietveld Method," *J. Am. Ceram. Soc.*, **81** [11] 2978-82 (1998).
  13. L. Barbieri, F. Bondioli, I. Lancellotti, C. Leonelli, M. Montorsi, A. M. Ferrari, and P. Miselli, "The Anortite-Diopside System: Structural and Devitrification Study. Part II: Crystallinity Analysis by the Rietveld-RIR Method," *J. Am. Ceram. Soc.*, **88** [11] 3131-36 (2005).
  14. T. Roisnel and J. R. Carvajal, "WinPLOTR: a Windows Tool for Powder Diffraction Patterns Analysis," *Mater. Sci. Forum*, **378** 118-23 (2001).
  15. B. W. Hakki and P. D. Coleman, "A Dielectric Resonator Method of Measuring Inductive Capacities in the Millimeter Range," *IEEE Microw. Theory Tech.*, **8** [4] 402-10 (1960).
  16. T. Nishikawa, K. Wakino, H. Tamura, H. Tanaka, and Y. Ishikawa, "Precise Measurement Method for Temperature Coefficient of Microwave Dielectric Resonator Material," *IEEE Microwave Theory Tech. Symp. Dig.*, **1** 277-80 (1987).
  17. A. Karamanov and M. Pelino, "Induced Crystallization Porosity and Properties of Sintered Diopside and Wollastonite Glass-Ceramics," *J. Eur. Ceram. Soc.*, **28** [3] 555-62 (2008).
  18. S. S. Jiang and K. F. Zhang, "Study on Controlling Thermal Expansion Coefficient of ZrO<sub>2</sub>-TiO<sub>2</sub> Ceramic Die for Superplastic Blow-Forming High Accuracy Ti-6Al-4V Component," *Mater. Design.*, **30** [9] 3904-7 (2009).
  19. R. Chen, Y. Wang, Y. Hu, Z. Hu, and C. Liu, "Modification on Luminescent Properties of SrAl<sub>2</sub>O<sub>4</sub>: Eu<sup>2+</sup>, Dy<sup>3+</sup> Phosphor by Yb<sup>3+</sup> Ions Doping," *J. Lumin.*, **128** [7] 1180-84 (2008).
  20. S. Rajesh, H. Jantunen, M. Letz, and S. Pichler-Willhelm, "Low Temperature Sintering and Dielectric Properties of Alumina-Filled Glass Composites for LTCC Applications," *Int. J. Appl. Ceram. Tech.*, **9** [1] 52-9 (2012).
  21. H. Wang, S. Xu, S. Zhai, D. Deng, and H. Ju, "Effect of B<sub>2</sub>O<sub>3</sub> Additives on the Sintering and Dielectric Behaviors of CaMgSi<sub>2</sub>O<sub>6</sub> Ceramics," *J. Mater. Sci. Tech.*, **26** [4] 351-54 (2010).
  22. B. K. Choi and E. S. Kim, "Effect of Crystallization Behavior on Microwave Dielectric Properties of CaMgSi<sub>2</sub>O<sub>6</sub> Glass-Ceramics," *J. Korean Ceram. Soc.*, **50** [1] 70-4 (2013).
  23. S. J. Penn, N. M. Alford, A. Templeton, X. Wang, M. Xu, M. Reece, and K. Schrapel, "Effect of Porosity and Grain Size on the Microwave Dielectric Properties of Sintered Alumina," *J. Am. Ceram. Soc.*, **80** [7] 1885-88 (1997).
  24. C. L. Lo, J. G. Duh, and B. S. Chiou, "Low Temperature Sintering and Crystallisation Behaviour of Low Loss Anorthite-Based Glass-Ceramics," *J. Mater. Sci.*, **38** [4] 693-98 (2003).
  25. A. Templeton, X. Wang, S. J. Penn, and N. M. Alford, "Microwave Dielectric Loss of Titanium Oxide," *J. Am. Ceram. Soc.*, **83** [1] 95-100 (2000).